Applied Ocean Research 97 (2020) 102085

Contents lists available at ScienceDirect

Applied Ocean Research

journal homepage: www.elsevier.com/locate/apor

Verification of a framework for cyclic p-y curves in clay by hindcast of Sabine River, SOLCYP and centrifuge laterally loaded pile tests

Youhu Zhang[a,*], Knut H. Andersen[a], Philippe Jeanjean[b]

[a] Norwegian Geotechnical Institute, Sognsveien 72, 0855 Oslo, Norway
[b] Upstream Segment Technical Authority for Geotechnical Engineering, Upstream Engineering Center, BP America Inc. 501 Westlake Park Blvd, Houston, TX 77079, United States

ARTICLE INFO

Keywords:
Pile
Clay
Cyclic lateral loading
p-y curves
Pile tests

ABSTRACT

Pile foundations supporting offshore structures, such as jacket platforms, are subjected to cyclic lateral loading. The capacity and deformation of these pile foundations under cyclic lateral loading are important and challenging design aspects. The purpose of this paper is to present verification of a framework for analysing the lateral pile response under cyclic loading in clay, based on fundamental soil behaviour measured in the laboratory at the element level. This framework can account for site-specific cyclic soil properties, summarized in classic contour diagrams, and the site-specific cyclic loading characteristics in design. This is a step-change improvement from current codes and standards recommendations which are based on a series of tests on a single pile at a single site (i.e. the Sabine River tests, Matlock 1962, 1970). The paper first provides a brief summary of the framework and outlines the important assumptions and calculation procedures. The paper then presents a comprehensive validation exercise of the framework through back-analyses of three sets of 1-g and centrifuge tests, covering different soil conditions (strength profile, OCR and plasticity) and loading sequences. This hindcast demonstrates the model's capabilities to capture the essential behaviours of pile foundations under cyclic lateral loading and its added value as a design tool, when compared with current practice.

1. Introduction

Offshore pile foundations typically need to be designed for cyclic lateral loading. As per state-of-practice, this is commonly performed by carrying out beam-column analyses where the soil pile interaction is represented by series of p-y springs (curves) along the depth of the pile. For both design and assessment, Jeanjean et al. [11] emphasized the importance of using best-estimate p-y curves which represent the soil support as accurately as possible. The most widely used p-y curves in clay are the API RP 2GEO curves [10] which were developed from limited pile tests at the Sabine River site in the 1950s, as reported in Matlock [21]. The API recommendations have essentially been unchanged since 1972 [4]. Their limitations are widely recognised in the industry and discussed amongst others in Jeanjean [10], Jeanjean et al. [11], and Zhang et al. [26]. In particular, the API method approximates the soil stress-strain response in monotonic and cyclic loading through the UU triaxial test. The project-specific cyclic loading conditions (e.g. make-up of storm load history, ratio between cyclic and average loading) are also not accounted for and the API cyclic curves are intended as minimum backbone curves obtained after several hundreds of cycles [20].

The industry lacks practical design procedures that can explicitly account for project-specific soil and load conditions. Zhu et al. [33] proposed an empirical p-y model that can account for the impact of the number of cycles and the cyclic loading amplitude on the evolution of the p-y curves based on two field pile load tests in soft clay. However, the consideration of site specific soil stress-strain response remains simplistic. The approaches presented by Erbrich et al. [8] and Zhang et al. [26,28] are two exceptions, which allow for consideration of project-specific soil and load conditions. The similarities and differences between the two models are discussed in Zhang et al. [26]. Zhang et al. [26,28] presented validation of their model through finite element analyses. The motivation of this paper is to present physical validation of the model through a comprehensive back-analysis exercise of several sets of field and centrifuge tests to demonstrate the model's ability to capture pile response under cyclic loading.

For completeness, the paper will first briefly describe the framework for calculating pile response under monotonic and cyclic pile head loading and will then report the back-analyses of the field and centrifuge tests.

* Corresponding author.
E-mail addresses: youhu.zhang@ngi.no (Y. Zhang), knut.h.andersen@ngi.no (K.H. Andersen), Philippe.Jeanjean@bp.com (P. Jeanjean).

https://doi.org/10.1016/j.apor.2020.102085
Received 20 September 2019; Received in revised form 21 December 2019; Accepted 2 February 2020

Notations

a	stress-strain curve fitting parameter
API	American Petroleum Institute
CPT	cone penetration test
D	pile diameter
DSS	direct simple shear test
E	elastic modulus
G_{max}	initial shear modulus
G_{50}	secant shear modulus at 50% strength mobilisation
GoM	Gulf of Mexico
I_p	plasticity index
m	SHANSEP model exponent
N	number of load cycles
NC	normally consolidated
N_{eq}	equivalent number of cycles
N_{eq_i}	equivalent number of cycles for the ith p-y spring along the pile
$N_{T\text{-}bar}$	T-bar factor for converting T-bar penetration resistance to soil undrained shear strength
UU	unconsolidated undrained triaxial compression test
OCR	over-consolidation ratio
p	lateral bearing pressure
p_a	average lateral bearing pressure
p_{cy}	cyclic lateral bearing pressure
p_u	ultimate lateral bearing pressure
P_{atm}	atmospheric pressure (100 kPa)
q_c	cone penetration resistance
s_u	undrained shear strength
s_{uC}	undrained shear strength measured in triaxial compression test
s_{uD}	undrained shear strength measured in direct simple shear test
s_{uE}	undrained shear strength measured in triaxial extension test
y	lateral displacement
z	soil depth
α	soil-pile interface roughness factor
γ	shear strain
γ_{cy}	cyclic shear strain
γ^e	elastic component of shear strain
γ^p	plastic component of shear strain
γ^{pf}	plastic component of shear strain at full strength mobilisation
ξ_1, ξ_2	coefficients for scaling p-y curve from stress-strain curve
σ'_v	effective in-situ vertical stress
τ	shear stress
τ_a	average shear stress
τ_{cy}	cyclic shear stress

2. Description of the model

2.1. The monotonic p-y approach

Zhang and Andersen [29] and Jeanjean et al. [11] proposed frameworks to derive site-specific monotonic p-y curves by scaling the soil stress-strain response measured in Direct Simple Shear (DSS) tests, as illustrated in Fig. 1. For a point on the normalised p-y curve with a mobilisation of p/p_u, the normalised lateral displacement y/D can be scaled from the strain evaluated at the same mobilisation ($\tau/s_u = p/p_u$) on the normalised stress-strain curve. Jeanjean et al. [11] showed that the two frameworks for scaling DSS curves into p-y curves give very similar results. The framework of Zhang and Andersen [29] was implemented in the beam-column software NGI-PILE and used in this work.

2.2. The cyclic p-y approach

Combining the concept of equivalent number of cycles N_{eq}, which is defined as the number of cycles at the current load level that would have produced the same cyclic effects (changes in strength and stiffness) as by the actual previous cyclic load history, Zhang et al. [26,28] extended the above monotonic framework to the cyclic p-y response of piles. On a single pile element level, it is postulated that the cyclic effects due to lateral loading of a pile element under pressure p_{cy} for N number of cycles is analogous to the shearing of a DSS soil element under stress τ_{cy} for N number of cycles if $p_{cy}/p_u = \tau_{cy}/s_u$, as illustrated in Fig. 2. By assuming so, a single N_{eq} can therefore be evaluated by the same strain accumulation procedure applicable for a DSS test, as described by Andersen [3]. For a pile element, if the previous loading history is equivalent to N_{eq} number of cycles at the current mobilisation level, the soil stress-strain response corresponding to N_{eq} can be derived from the cyclic strain contour diagram, which is established from cyclic soil element testing. By using the same scaling procedure used for monotonic p-y curves (i.e. [29]), the p-y curves for calculating the pile responses under the current cyclic loading can be derived.

Fig. 3 provides a schematic illustration of the concept. The figure illustrates a pile element with a combination of average and cyclic mobilisations equal to 0.2 and 0.4 of the static capacity, respectively, and a $N_{eq} = 10$. Note that the cyclic mobilisation is defined as the mobilized soil pressure under the cyclic component of the pile load normalized by the ultimate static bearing pressure for the pile element in consideration. Similar definition applies to the average mobilisation level. The stress strain curves for average and cyclic components of loading can then be established by drawing a horizontal cross-section at $\tau_{cy}/s_u = 0.4$ and a vertical cross-section at $\tau_a/s_u = 0.2$ respectively. The

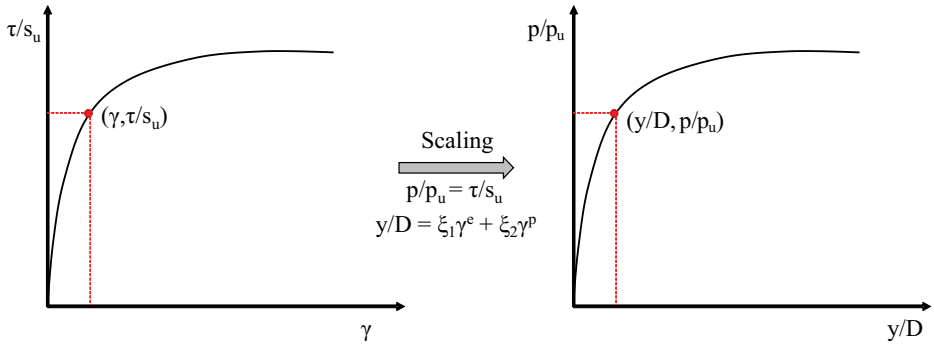

Fig. 1. Illustration of framework for deriving monotonic p-y curves from stress-strain response measured in DSS tests [11,29].

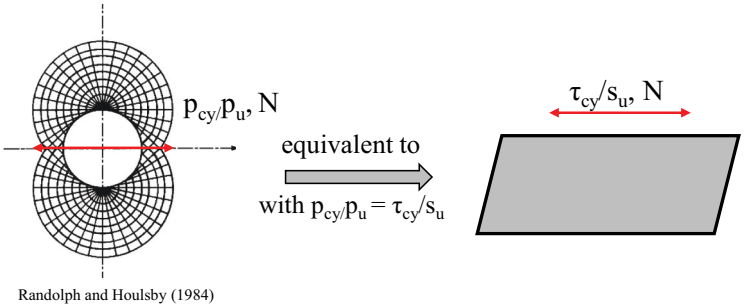

Fig. 2. Analogy between loading of a pile element and shearing of a DSS soil element [26].

cross-section lines intersect with the average or the cyclic strain contour lines, and the intersection points form the stress-strain curves.

Using these p-y curves, the pile response under the current load can be evaluated. Note that the total pile response (displacements and forces) is the sum of responses under average and cyclic components of the pile load. With the above assumptions, the pile response under a pile head load history can be analysed within the framework of a conventional beam-column p-y model, as schematically illustrated by Fig. 4. The design pile head load history is first sorted into load parcels with constant average and cyclic loads. The load history is then analysed in a parcel by parcel manner. The key is to keep track of the loading history for each of the p-y elements. By updating the global equilibrium and p-y springs at the beginning and at the end of each load parcel, the evolution of the pile response during the load history can be calculated. This procedure is explained in detail in Zhang et al. [28] and implemented in a computer program called NGI-PILE.

The cyclic framework described above has been validated by numerical analyses, firstly at a single pile element level (i.e. a horizontal pile slice) to verify the analogy illustrated in Fig. 2, and then for a complete pile to verify the calculation procedure and redistribution of loads along the pile under cyclic loading. These were performed in finite element analyses with the UDCAM cyclic accumulation soil model [12], which uses cyclic contour diagrams established from soil elements tests as input. In the analyses, the stress history at each integration point of the entire finite element soil domain was kept track of and the soil strength and stiffness at each point is constantly updated. The numerical validation exercise demonstrates excellent predictive capability the model and further details can be found in Zhang et al. [26,28].

2.3. Modelling of the pile-soil interface

The proposed model allows for explicit consideration of the pile-soil interface roughness. The interface roughness not only influences the ultimate capacity of the p-y spring [27], but also the stiffness [29]. The user of the model can therefore evaluate the interface roughness based on the soil profile, for example, according the axial capacity method recommended in API [5]. This also allows for the possibility to account for the effect of the pile installation method, which has an important

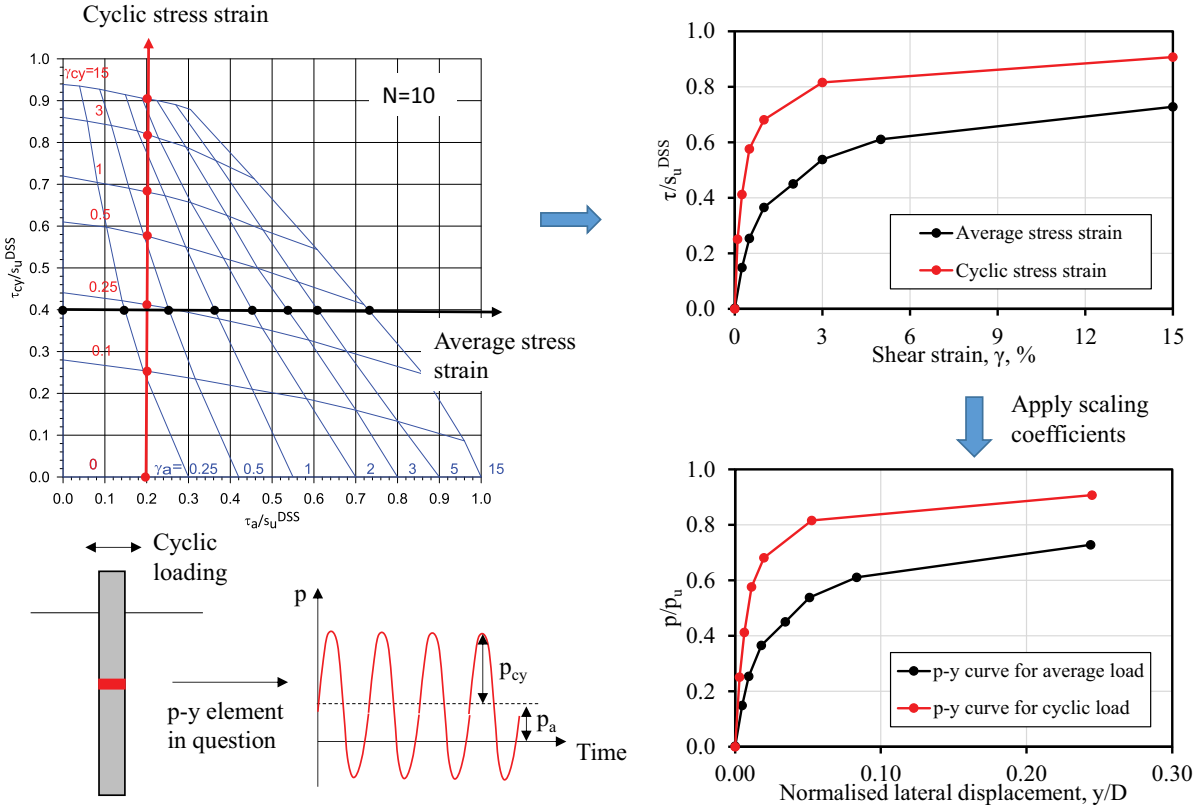

Fig. 3. Schematic illustration on derivation of p-y curves for average and cyclic components of loading (modified from [28]).

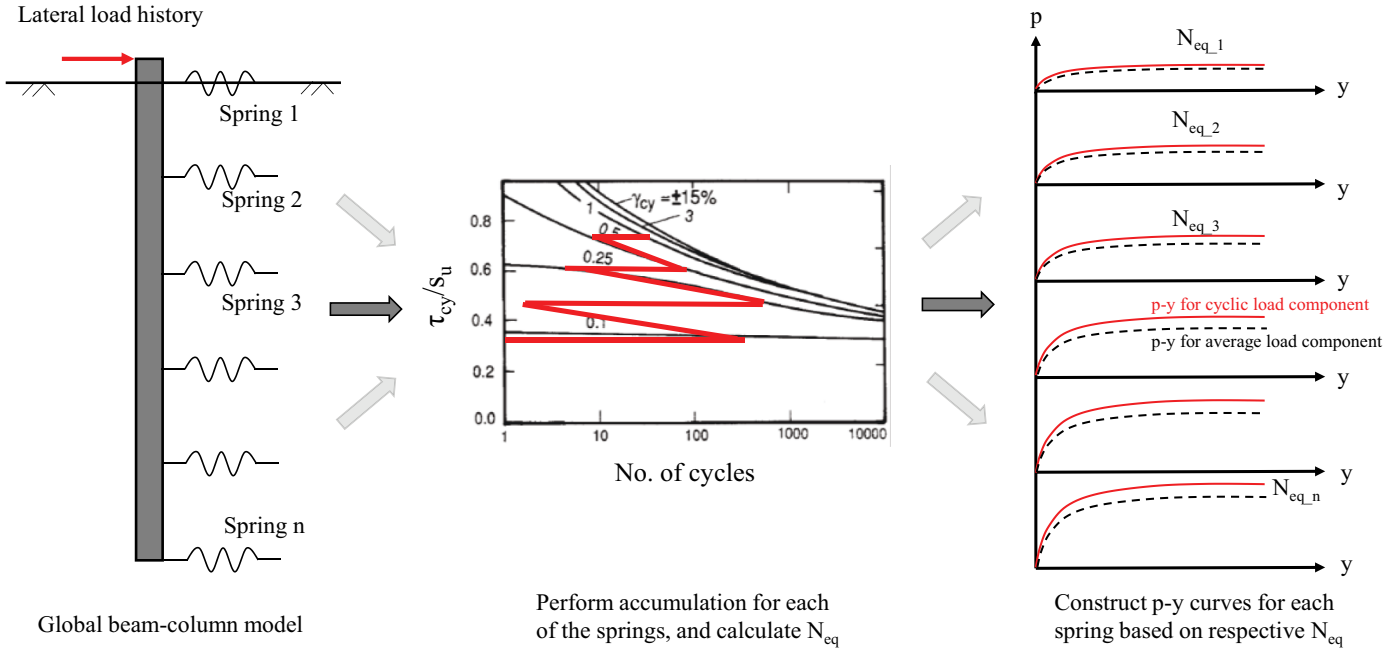

Fig. 4. Schematic illustration of general procedure to analyse an entire pile response [28].

impact on the soil properties around the pile shaft. This is particularly relevant to the axial pile capacity and load-displacement response. It also influences the lateral response, despite to a less extent because the lateral response is more dominated by the soil outside the immediate influence zone of pile installation. In the proposed framework, the effect of the pile installation method can be approximated by choosing an appropriate interface roughness factor.

2.4. Limitation

It should be noted that the monotonic and cyclic p-y framework outlined above is primarily developed for design of slender piles where the soil-pile interaction can be sufficiently captured by distributed p-y springs along the pile and a flow-around soil mechanism is dominating. For short stubby piles, such as monopiles supporting offshore wind turbines, additional components of soil resistance, such as base shear at pile tip and distributed moment due to vertical shear force along pile shaft, also need to be considered [6,32].

3. Validation of the model against physical pile testing

3.1. Overview

Several field and centrifuge tests reported in the literature are back-analysed in order to verify the proposed cyclic p-y framework. This includes the Sabine River tests [19], which formed the basis for development of the API p-y curves [21], the centrifuge experiments reported in Zakeri et al. [25], the SOLCYP centrifuge experiments reported in Khemakhem [14], and the Haga pile load tests [13]. In this paper, the back-analyses of these tests using the proposed p-y framework are reported, except for the Haga pile tests for which the readers are referred to Zhang et al. [30] for an extensive documentation of their hindcast. For each testing programme, the details of the tests (geometry, instrumentation, soil conditions) are first briefly described. The monotonic and cyclic stress-strain responses of the soil are then evaluated. Lastly, monotonic and cyclic loaded pile tests are back calculated and compared to observed pile behaviours.

Note that Jeanjean et al. [11] already presented a comprehensive back-analysis of those monotonic tests that will be reported below using "default" sets of monotonic p-y curves, one for natural clays and one for kaolin. This paper presents a refinement of those back-analyses by (1) using site-specific p-y curves derived from site-specific soil stress-strain responses accounting for OCR effect, (2) using slightly modified shear strength profiles, and (3) accounting for rate effects on the soil shear strength (i.e. taking in to account the difference in time to failure between the DSS tests and the monotonic pile tests).

3.2. Sabine River field pile testing

3.2.1. Geometry and instrumentation

The Sabine River pile load tests are summarized in Matlock and Tucker [19] and analysed in Matlock [20]. These tests formed the primary basis of the "Matlock p-y formulation" in soft clays [21], which was adopted by API RP2A 3rd Edition [4] and still appears in API RP 2GEO [4]. The model pile had an outer diameter of 0.324 m, a uniform wall thickness of 12.7 mm, and a total length of 13.1 m. The pile was embedded 12.8 m below the ground surface so that the lateral load was applied 0.3 m above the ground surface. The model pile was instrumented with 35 pairs of strain gauges which measured the bending moment along the pile. The spacing between the gauges varied from 0.15 m near the top to 1.22 m in the lowest section.

The model pile was driven closed-ended to the target penetration by impact hammering. Four main tests were carried out at the Sabine River site, including two monotonic loading tests (one free head and one constrained head) and two cyclic loading tests (one free head and one constrained head). Due to the uncertainty with the exact level for fixity for the constrained pile head tests, only the two free head tests are back-analysed in the current exercise.

3.2.2. Soil condition

The tests were carried out at a site near the Sabine River mouth, which primarily consists of marine-deposited, high plasticity clay, but interbedded with thin silty sand and sand layers. A desiccated 1.38 m thick surface crust was excavated, below which a soft marine clay of high plasticity with water content close to the liquid limit values was present to a depth of 3 m. A clay with 25 mm to 100 mm thick seams of shelly sand occurred between depths of 3 m and 4 m and a silty sand with numerous shell fragments but enough clay to provide an effective matrix was present between depths of 4 m and 5 m. A clean sand layer occurred between depths of 5 m and 6 m, and below 6 m, the soil

consisted of high plasticity clay similar to the soil in the upper 3 m, but with greater strength due to higher consolidation stress.

Fig. 5 illustrates the site investigation results. The results of unconfined compression tests are consistently lower than those of the vane and were not relied upon by Matlock [20] when establishing the shear strength profile. Fig. 5 illustrates the strength profile adopted by the current back-analysis, which is consistent with those of Matlock [20] and Jeanjean et al. [11] despite some minor simplifications near the surface (Fig. 5). The current back-analysis neglects the sandy layers between 13 and 20 feet (4–6 m) below the ground surface and assumes a continuous undrained shear strength profile within this depth interval, where significant scatter of vane results is seen. The undrained shear strength profile is taken to be representative of strength measured in DSS tests. It remains constant at 13 kPa from ground surface to 2 m depth and then increases linearly with depth at a gradient of 1.54 kPa/m. The submerged unit weight of the soil was not reported and is estimated to be 6 kN/m^3. The plasticity index (I_p) for the surface plastic layer is between 50–70%, which is similar to typical GoM material.

The over-consolidation ratio (OCR) of the soil at the test site is estimated using the SHANSEP method [15]:

$$s_u = \left(\frac{s_u}{\sigma'_v}\right)_{NC} \mathrm{OCR}^m \tag{1}$$

Assuming a $(s_u/\sigma'_v)_{NC}$ ratio of 0.25 and $m = 0.8$ based on typical values for Gulf of Mexico clay [16], the OCR is estimated using Eq. (1) together with the s_u profile recommended for back-analysis as illustrated in Fig. 5. It can be seen that and the OCR decreases rapidly with depth from around 20 at 1 m below excavated ground surface to 2 at 10 m depth. A simplified stepwise OCR profile, as illustrated in Fig. 5 is used in the back-analyses. This point will be further discussed.

For the back-analyses, the pile-soil interface roughness factor (α) was estimated using the method recommended in API RP 2GEO [5] for calculating the axial shaft friction of driven piles in clay:

$$\alpha = 0.5\left(\frac{s_u}{\sigma'_v}\right)^{-0.5} \text{ for } s_u/\sigma'_v \le 1.0$$
$$\alpha = 0.5\left(\frac{s_u}{\sigma'_v}\right)^{-0.25} \text{ for } s_u/\sigma'_v > 1.0 \tag{2}$$

The value of α is between 0 and 1.0. Based on the above equation, an average interface roughness factor of 0.6 is estimated and was used in the back-analysis.

According to the empirical guidance from Jeanjean et al. [11], a gap is expected to open on the back side of the pile during lateral loading and indeed was observed during cyclic testing (gap formation was not documented for the static tests). Presence of a gap is therefore assumed in the back-analyses. The effect of shear strength anisotropy on the ultimate lateral bearing capacity for the wedge failure was accounted for according to the method suggested in Jeanjean et al. [11]. A typical anisotropy ratio (s_{uE}/s_{uD}) (triaxial extension strength over DSS strength) for GoM clays of 0.9 was assumed.

3.2.3. Monotonic and cyclic stress-strain behaviour

The back-analyses assume that the monotonic and the cyclic stress-strain behaviours of the Sabine River clay are similar to those of GoM clays. Zhang et al. [28] presented the DSS monotonic and the cyclic properties of normally consolidated GoM clay (i.e. OCR = 1) based on

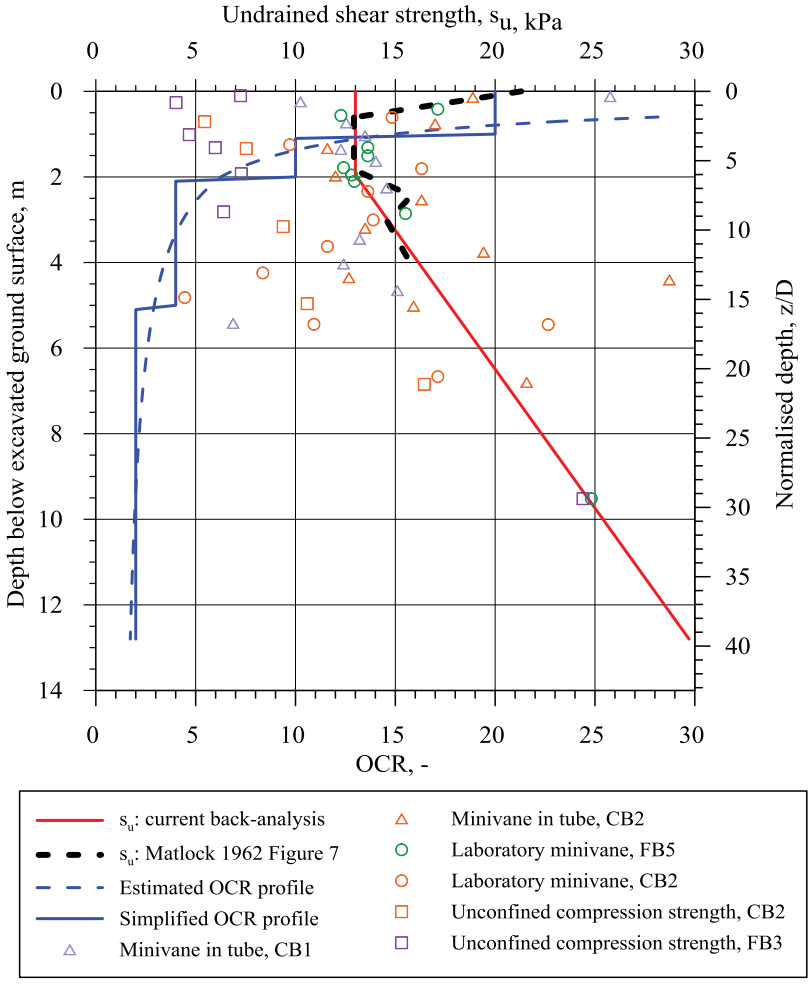

Fig. 5. Undrained shear strength profile and over-consolidation ratio with depth ($z = 0$ refers to excavated ground surface).

an extensive database from ten sites in the GoM. Reference is made to Zhang et al. [28] for the details. For completeness, Fig. 6 presents the cyclic strain contour diagrams for normally consolidated GoM clays under DSS shearing mode. Each point on the contour diagram represents the average and cyclic shear strains that are developed on a DSS soil element when it is cyclically loaded under the corresponding average and cyclic shear stresses for the specified number of cycles.

3.2.3.1. Correction for OCR effect on the stress-strain behaviour. It is well understood that higher OCR leads to more ductile stress-strain response due to dilative behaviour of high OCR clays, which requires larger strains to mobilise its strength. This is illustrated by for example triaxial tests of reconstituted kaolin [23] and DSS tests of Drammen clay [3] on samples consolidated to different OCRs. Jeanjean et al. [11] reports a database of 537 DSS stress-strain curves that was compiled from tests on samples from 5 offshore regions which also reveals a clear trend, as illustrated in Fig. 7.

As illustrated by Fig. 5, the soil at the Sabine River is over-consolidated, although the OCR reduces rapidly with depth. However, due to the small diameter of the pile tested (0.324 m), the effect of OCR should be taken into account when back-analysing the field test results. Since the monotonic and cyclic properties of over-consolidated GoM clay are not available, the OCR effect is accounted for in an empirical manner here. Fig. 8 shows the ratio of normalised secant shear modulus value at 50% strength mobilisation (G_{50}/s_{uD}) measured in DSS test between over-consolidated specimen and normally consolidated

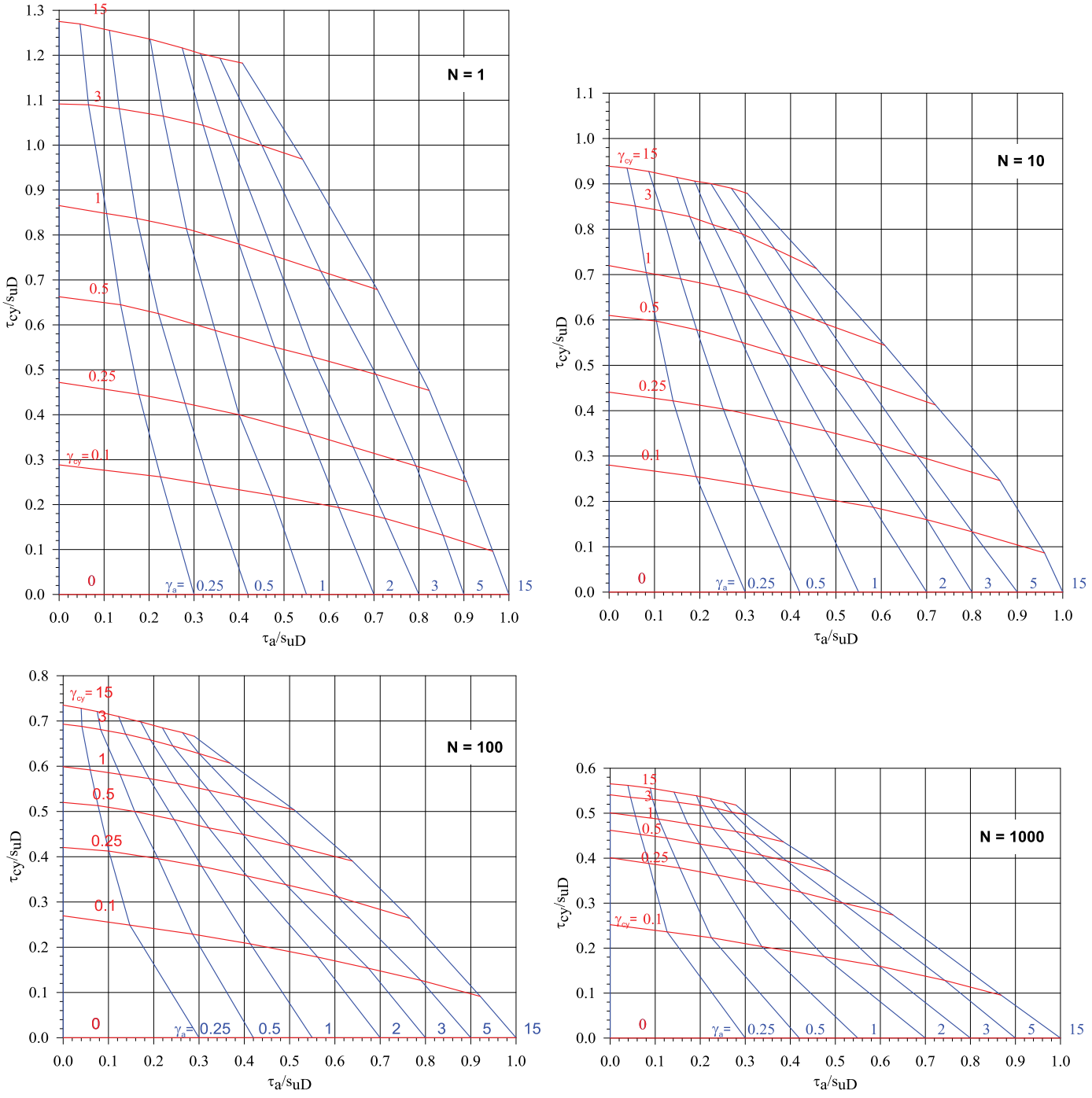

Fig. 6. Cyclic strain contour diagrams for normally consolidated GoM clay under DSS shearing mode.

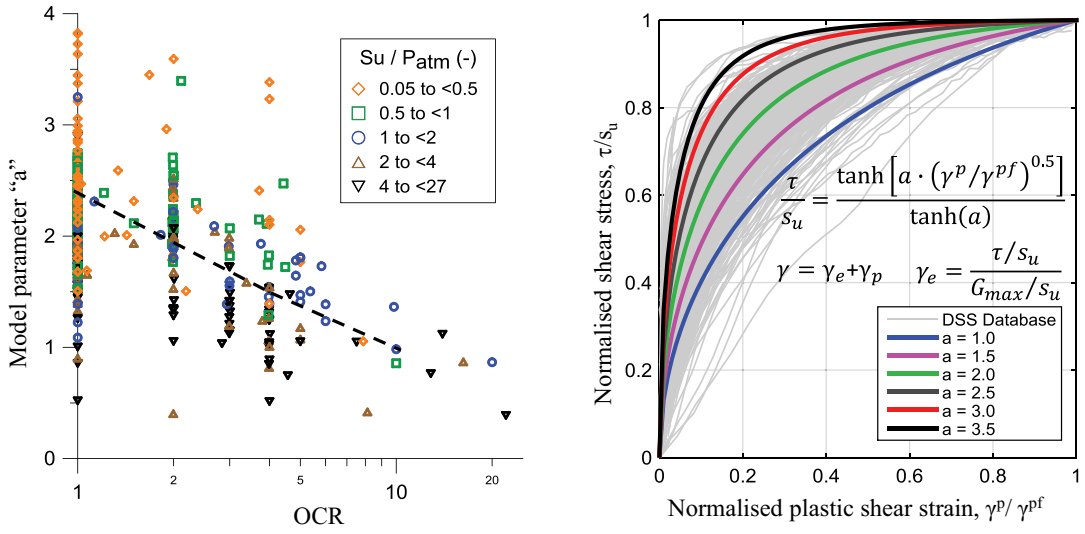

Fig. 7. Effect of OCR on normalised stress strain response (adapted from Jeanjean et al. [11], a decreasing parameter "a" indicates a more ductile normalised stress-strain curve).

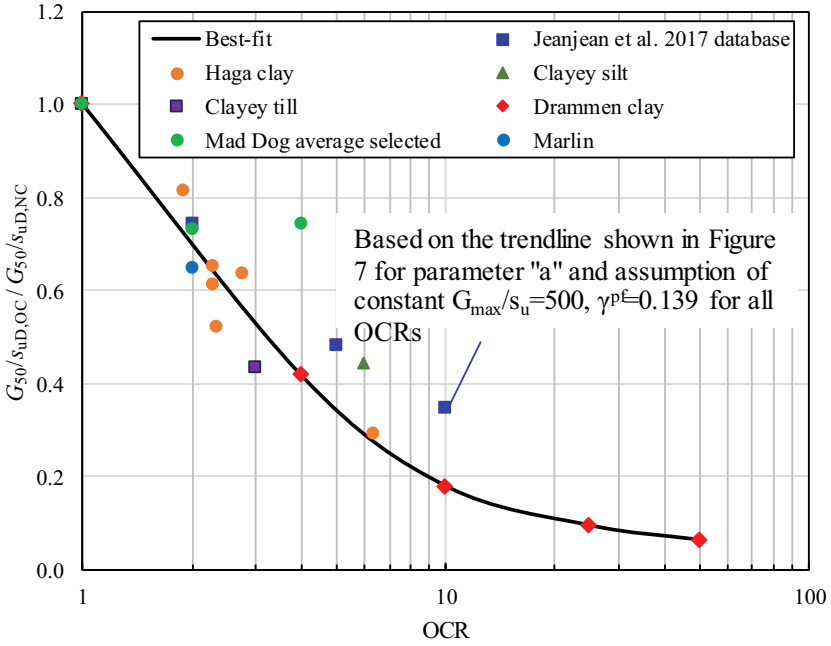

Fig. 8. Effect of OCR on $G_{50}/s_{uD,OC}$/ $G_{50}/s_{uD,NC}$.

specimen for several different clayey soils as well as the trend suggested by the Jeanjean et al. [11] database (the data points shown in the figure were evaluated based on a parameter "a" following the trend line shown in Fig. 7, an assumed constant G_{max}/s_u ratio of 500 and γ^{pf} value of 0.139 for all OCRs). The G_{50}/s_{uD} ratio clearly decreases with increase of OCR. All the data appears to agree reasonable well, despite that the trend suggested by the Jeanjean et al. [11] database plots slightly higher, which is believed due to the assumption of constant G_{max}/s_u and γ^{pf} values, resulting in underestimation of the stiffness for normally consolidated soils and over-estimation of the stiffness for over-consolidated soils. To account for the effect of OCR, the G_{50}/s_{uD} ratio between over-consolidated soil and normally consolidated soil implied by the best-fit line drawn in Fig. 8 is used to scale the strain values in the monotonic stress-strain response and in the cyclic strain contour diagrams to derive soil responses for over-consolidated soils. It should be noted that this is an approximate way to account for the OCR effect. At very small strains, the impact of OCR is less. The correction applied hereby may thus result in too soft initial response at low mobilisation levels. Fig. 9 presents the monotonic stress-strain curves for different OCRs scaled from that for normally consolidated GoM clay and corresponding p-y curves that were used in the back-analysis.

3.2.4. Back analysis of monotonic test

The normalised monotonic p-y curves presented in Fig. 9 were used. Two back-analyses were performed: analysis no.1 uses the undrained shear strength profile as illustrated in Fig. 5; and analysis no. 2 with a factor of 1.3 applied to the undrained shear strength profile. The 1.3 factor accounts for the rate effect due to the difference in rate of loading between the DSS tests and the pile load test, as discussed below.

Fig. 10 presents the results of the back-analyses in comparison with the measured response. From the inserted plot it can be seen that the back-analysis without considering the strain rate effect considerably over-estimates the pile head deflection (measured 0.3 m above test ground surface). On the other hand, the back-analysis with rate effect

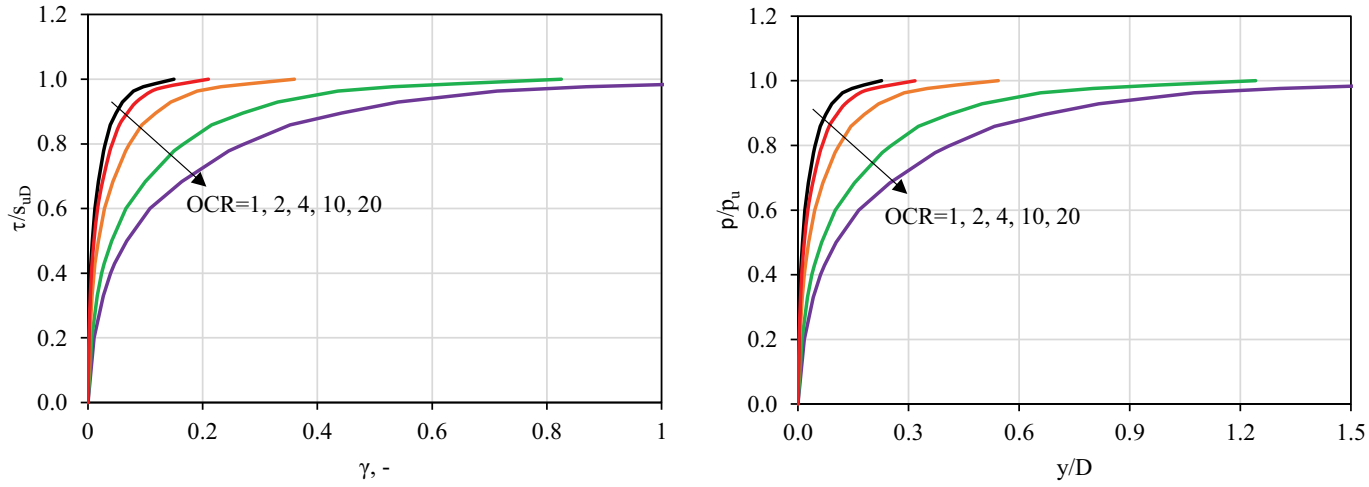

Fig. 9. Monotonic stress-strain (left) and corresponding p-y curves (right) used in back-analysis (an interface roughness factor $\alpha = 0.6$ is used for deriving the p-y curves from stress-strain curves).

yields a much improved match with the measured response. This comparison raises an important aspect that need to be considered between laboratory soil element test and field or model pile tests in general. The laboratory monotonic DSS test is typically carried out at a constant shear strain rate of about 5% per hour. Consider a failure strain of 15% for the GoM soil, this means 3 h to failure. In the field/model testing, such extended loading time is generally not used. With regard to the Sabine River test, the pile head load was applied in 5 increments. The exact duration of each load increment is unknown, and the factor of 1.3 is thus uncertain. However, considerable rate effect relative to the laboratory strain rate is expected. This may partially explain why the back-analysis without the rate effect predicts softer response than measured. The negligence of the sandy layers between 4–6 m may have also contributed to the difference.

Fig. 10 also presents a comparison of the lateral deflection and bending moment profiles along the pile between the back-analysis and the measured response for the free head monotonic loading test at five different pile head load levels. The results of back-analysis with rate effect are presented. A reasonably good match is demonstrated.

Table 1
Summary of cyclic load history of the free head cyclic test.

Parcel	No. of cycles	Min load, kN	Max load, kN	Ave. load, kN	Cyc. load, kN
1	400	−8.9	17.8	4.45	13.35
2	200	−8.9	35.6	13.35	22.25
3	200	−8.9	53.4	22.25	31.15
4	200	−8.9	60	25.55	34.45

3.2.5. *Back analysis of cyclic test*

Table 1 summaries the load history of the Sabine River free head cyclic lateral load test. The load history consists of four load parcels. Within each parcel, the cyclic loading remains constant. The load level increases with the parcel number. Except Parcel 1, all the remaining three parcels have 200 load cycles. The period for each load cycle is 20 s,

Fig. 11 presents the results of the back-analysis, including the evolution of sectional bending moment and the lateral deflection along the

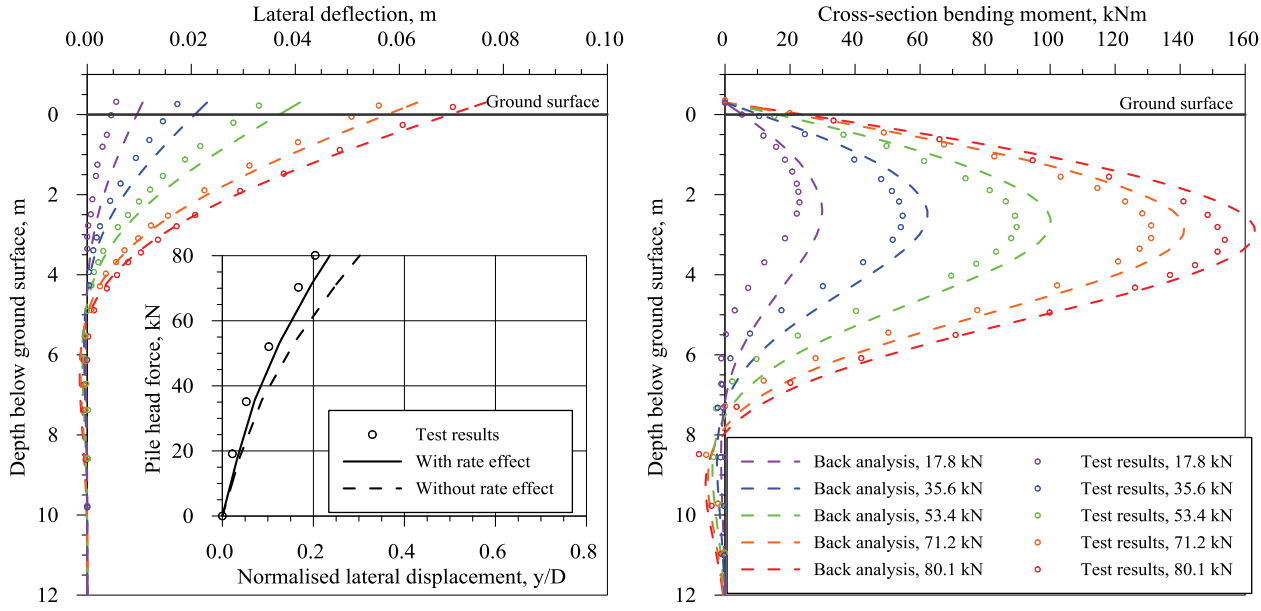

Fig. 10. Measured versus back-analysed pile response in the Sabine River free head monotonic test.

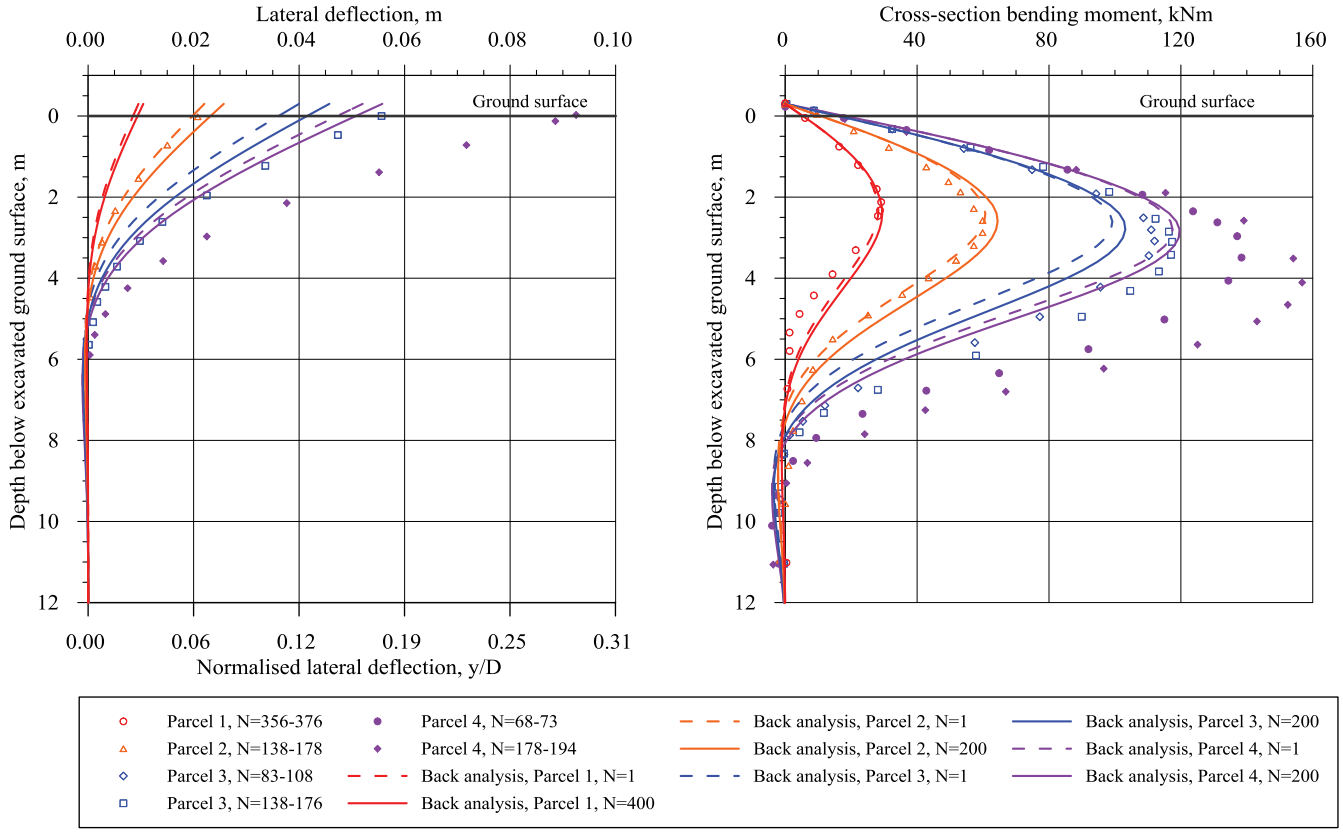

Fig. 11. Back-analysis of the Sabine River free head cyclic test.

pile with cyclic loading. Test results, where available, are presented for comparison. It should be noted that the test results are based on readings of peak strain gauge values during continuous cyclic loading. The results along the depth do not correspond to a given moment, but for a given period, as indicated by the legend. The change of the values during the time period is assumed to be small as the readings were typically taken when cyclic degradation had stabilised in each parcel. The agreement between the test results and the back-analyses is very good for the first two load parcels. However, from parcel 3, the model predicts stiffer response than the behaviour actually observed. In parcel 4, the model predicts a pile response that becomes stabilised and exhibits limited degradation with cyclic loading. In comparison, the field test suggests significant degradation in stiffness and large increase in bending moment. One important aspect that is believed to contribute to the large difference between back-analysis and test observation in parcel 3 and parcel 4 is the progressively developed permanent displacement of soil away from the pile. Under the lateral loading, the soil in front of the pile is pushed away and a cavity is formed behind the pile due to permanent soil deformation. Although the cavity is only measured in the end of the cyclic test, it is postulated that the cavity grows in size and depth as the cyclic loading progresses. During a load cycle, the pile feels no soil resistance until it is pushed far enough to close up the gap again. This causes an apparent “degradation” of the soil-pile interaction stiffness. However, this phenomenon is not captured by the current model, which is fundamentally based on a flow-around soil mechanism. Although the current model accounts for tension gap opening partially by reducing the ultimate strength of the p-y curve, it assumes that soil follows the movement of the pile, and the decrease of the soil-pile interaction stiffness predicted by the model is entirely due to the degradation of the soil.

However, it is important to reflect on the significance of the above discrepancy between model prediction and field observation for the practical design of offshore piles for oil and gas platforms. There are two points to be noted:

1) In the cyclic pile tests at Sabine River, four parcels of constant amplitude cyclic loading were consecutively applied to the pile head. The cyclic load amplitude increased consecutively. In the largest load parcel, the peak horizontal load would have resulted in more than 10% pile deflection at ground surface if the load had been applied monotonically. This represents an extremely high load level. 200 cycles were applied in each load parcel, except the first one, where 400 cycles were applied. This differs significantly from the actual load history encountered by pile foundations supporting offshore structures. Zhang et al. [31] suggests that the equivalent number of cycles along a pile foundation supporting a jacket structure in Gulf of Mexico and the North Sea is typically less than 25.
2) A mudmat is typically placed on the soil surface, enclosing a pile or a pile group at each corner of the legs supporting a jacket structure. The mudmats are designed to support the jacket structure prior to piling, but it also acts as a seal and cuts off the seepage path for water getting into the pile-soil interface during cyclic loading. The soil is then forced to adhere to the movement of the pile. The gapping mechanism, which led to the “apparent degradation” of soil-pile interaction stiffness in the Sabine River test, is thus considered unlikely to occur in practice, even for piles in stiff clay.

In summary, the limitations of the model in predicting the Sabine River cyclic test results for the very large displacement levels and number of cycles is not deemed critical for the design of oil and gas platforms.

3.3. Zakeri et al. [25] centrifuge model testing

3.3.1. Geometry and instrumentation

The centrifuge tests were performed at 55.35 g. The model pile had a diameter of 17.4 mm and a wall thickness of 0.92 mm and was made of grade 4140 steel. It was equipped with 18 levels of strain gauges to measure the bending moment profile along the pile. Due to the epoxy coating on the strain gauges, the diameter of the pile was slightly increased. In prototype scale, the pile had an outer diameter of 0.963 m, an inner diameter of 0.879 m and a wall thickness of 42 mm. All the results are reported in prototype scale below, unless otherwise stated.

The model pile was installed through a predrilled hole at 1 g upon completion of lab floor consolidation of the soil sample. The soil was further consolidated at testing g level in the centrifuge. A final pile embedment depth of 25.74 m was achieved. During the pile tests, the displacement-controlled loading was applied through a pin connection located at 4.76 m above the ground surface.

3.3.2. Soil condition

The centrifuge experiments were carried out in lightly over-consolidated Kaolin clay. Fig. 12 illustrates two mini T-bar test results and interpreted undrained shear strength profile, using a $N_{T\text{-bar}}$ factor of 10.5. Shallow correction presented by White et al. [24] was applied in interpretation of the strength in the upper 1.1 m (20 mm in model scale, which corresponds to 2.5 T-bar diameters in the centrifuge). According to Low et al. [17], $N_{T\text{-bar}} = 10.5$ would for typical natural clays give the triaxial compression strength. Therefore, the strength profile presented in Fig. 12 is taken to be the triaxial compression strength. Andersen et al. [2] reports $s_{uD}/s_{uC} = 0.9$ for Kaolin clay. This anisotropy ratio was assumed to derive the DSS strength for the back-analysis presented below.

Due to the very low undrained shear strength at mudline, no tension gap was observed in the centrifuge tests. The back-analyses presented below therefore assumed no gapping. Furthermore, a fully rough pile-soil interface roughness was considered.

3.3.3. Stress-strain responses under monotonic and cyclic shear stresses

There were no cyclic soil element tests carried out on the Kaolin clay used in the centrifuge experiments. The Kaolin clay cyclic properties used in this back-analysis were based on a collaborative study between the University of Western Australia (UWA) and the Norwegian Geotechnical Institute (NGI), as reported in Carotenuto et al. [7]. All the DSS tests were performed at NGI on normally consolidated Kaolin, prepared from the PRESTIGE-NY Kaolin powder, supplied by Sibelco Australia. This Kaolin is widely used for centrifuge model testing at UWA and hence is referred as UWA Kaolin clay hereafter. The plasticity index (I_p) of the UWA Kaolin clay is measured to be 28%.

The monotonic DSS stress-strain response of kaolin reported by Jeanjean et al. [11] was complemented by five additional monotonic tests carried out at NGI on UWA kaolin to augment the database as properties of the kaolin clay can vary between suppliers.

3.3.3.1. Monotonic stress-strain behaviour. Five monotonic DSS tests were carried out on normally consolidated UWA Kaolin with a shear strain rate of 4.7% per hour. The results were very repeatable. Fig. 13 presents the representative normalised stress-strain curves of the UWA Kaolin and the p-y curve constructed using an interface factor $\alpha = 1.0$, which was used in the back-analysis below. The initial stiffness of the normally consolidated UWA kaolin was estimated from the stiffness degradation curves measured in the five monotonic DSS tests by extrapolating to small strains. A $G_{max}/s_{uD} = 500$ is estimated.

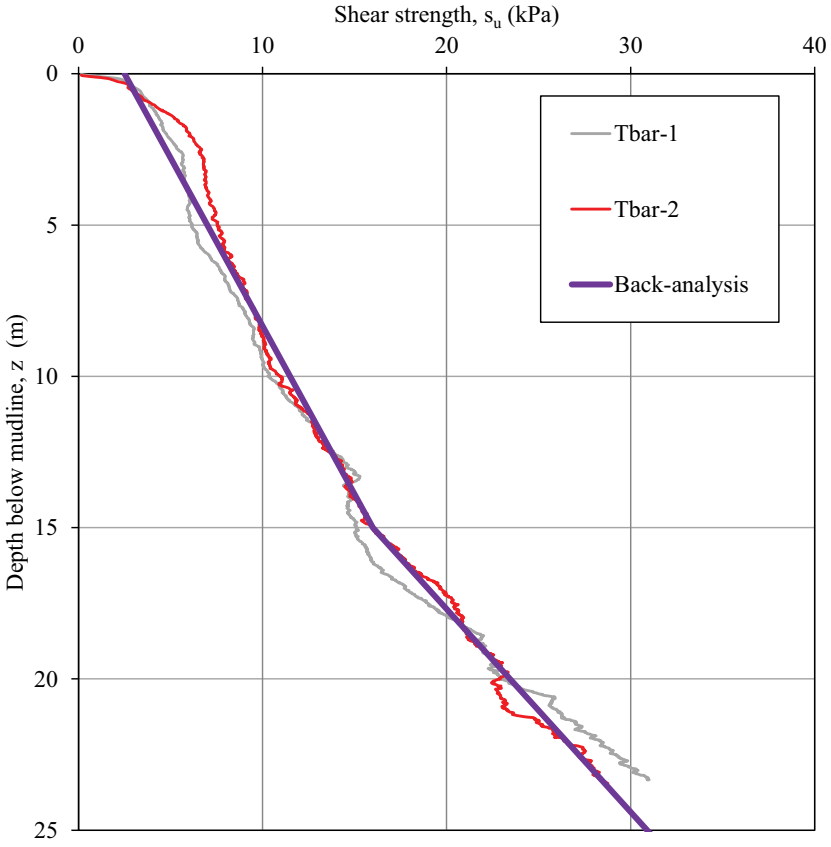

Fig. 12. Undrained triaxial compression shear strength profile of Zakeri et al. [25] centrifuge tests.

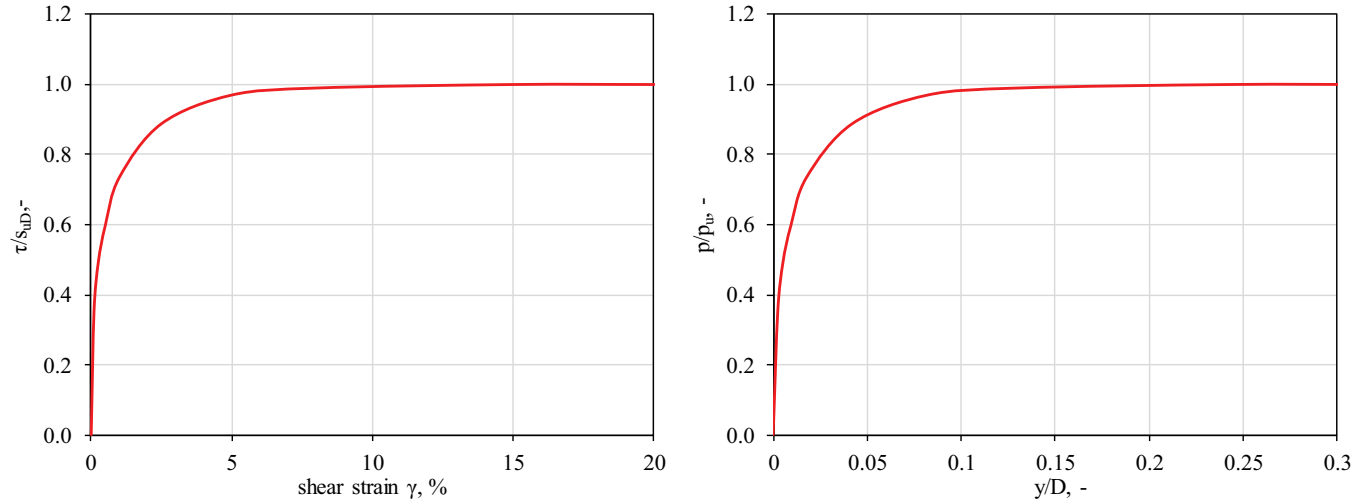

Fig. 13. Monotonic stress-strain response of normally consolidated UWA Kaolin clay and corresponding monotonic p-y curve for an interface factor $\alpha = 1.0$.

3.3.3.2. Cyclic contour diagrams. In total 11 cyclic DSS tests were carried out on normally consolidated UWA kaolin to develop the cyclic interaction diagrams. These tests cover different combinations of normalised average and cyclic shear stresses. Further details on those cyclic DSS tests and the cyclic contour diagrams can be found in Carotenuto et al. [7]. Compared with Drammen clay [1], the UWA kaolin degrades faster with number of load cycles.

3.3.4. Back-analysis of monotonic test

The monotonic test was performed displacement controlled at a rate of circa 8% pile diameter per second, which is approximately 3 orders of magnitude higher than a typical laboratory DSS test. To account for the increase in shearing rate between the DSS test and the pile test, the shear strength was increased by 25% in the back analysis. This correction is in the low range of the rate effect data base presented by Lunne and Andersen [18].

Fig. 14 presents the measured and back-analysed lateral deflection and bending moment profile with depth at three different pile head load levels as well as the pile head load-displacement response for the monotonic push-over test, with good agreement.

3.3.5. Back-analysis of cyclic tests

Two cyclic pile tests under harmonic displacement cycles are back-analysed. The cyclic displacement motions were applied to the pile head, and the horizontal force exerted to the pile head was measured. In each test, a series of motions with different displacement amplitudes were applied consecutively, with three months, in prototype units, waiting period in-between two cyclic motions. Each displacement motion consisted of 1000 cycles. Table 2 summaries the applied displacement motions in those two tests. In Test C2, the displacement is symmetric (i.e. two way cycling) and the cyclic amplitude increases with motion number, except the last one. In the back-analysis presented below, each motion is treated as an independent test, i.e. assuming the previous loading history is totally erased due to higher load level applied in the current motion. Apparently, this does not hold for Motion M2b, which was therefore not back-analysed. In Test C3, M1 is a two way symmetric cycling. However, in motion 2–5, an average displacement component (offset) is introduced. Since the total displacement amplitude in motion 4 is reduced from motion 3, only the first three motions in this test were back-analysed, assuming each motion as an independent cyclic test.

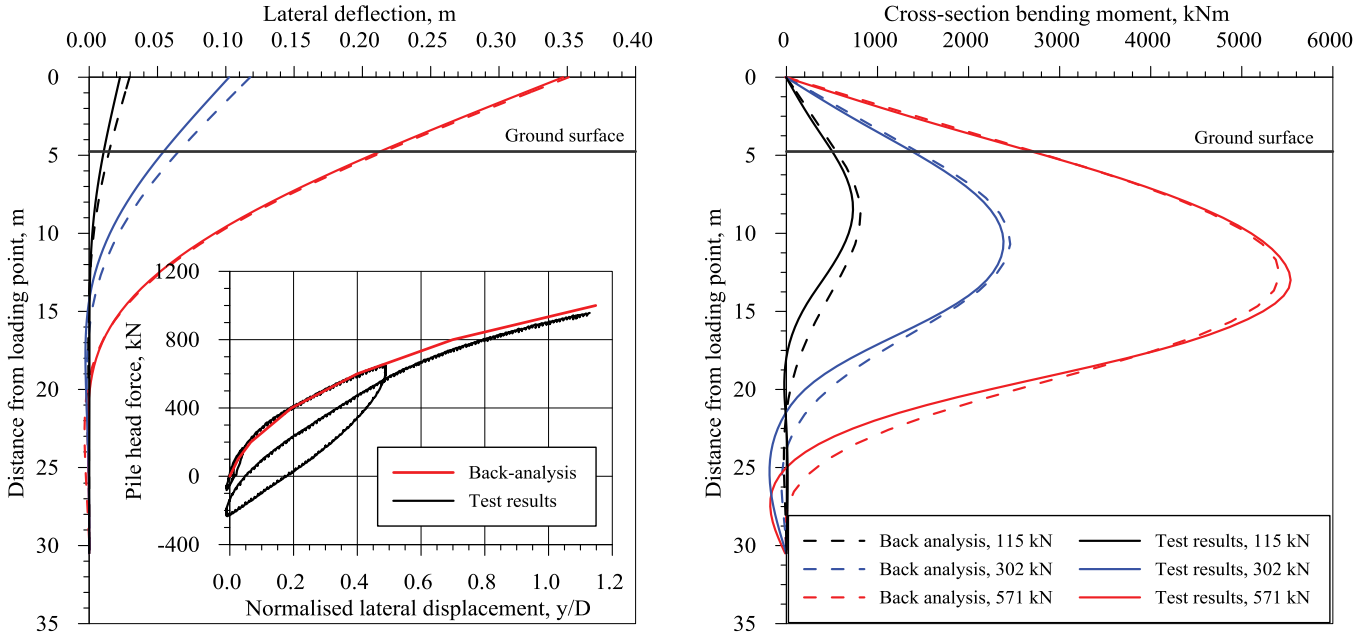

Fig. 14. Back-analysis of the monotonic test (pile head displacement measured at the load application point).

Table 2
Summary of displacement motions.

Test	Motion	Offset	Amplitude*
C2	M1	0	0.025D
	M2	0	0.05D
	M3	0	0.10D
	M4	0	0.15D
	M5	0	0.25D
	M2b	0	0.05D
C3	M1	0	0.025D
	M2	0.05D	0.05D
	M3	0.05D	0.10D
	M4	0.05D	0.025D
	M5	0.10D	0.025D
	M6	0	0.10D
	M7	0	0.15D

* Amplitude is defined as half of the distance between the peak and the trough.

The cyclic motions were applied with a frequency of 1 Hz. However, the cyclic contour diagrams were based on DSS tests that were carried out at a frequency of 0.1 Hz. The loading rate in the pile test is therefore 10 times higher. To account for this difference, a factor of 1.08, based on the database presented by Lunne and Andersen [18], was applied to scale up the cyclic shear stresses on the strain contour diagrams, while the average shear stresses are not scaled.

Since the cyclic tests were performed under displacement control, the exerted lateral load at pile head reduced as cycling proceeded due to cyclic degradation. Rapid degradation was observed for the first 100 cycles, and the response became gradually stabilised after that. However, as the cyclic p-y model is developed based on loads as input, the measured pile head lateral load history was idealised into constant amplitude load parcels, which were then used in the back-analysis. Fig. 15 shows an example, in which the evolution of the pile head load with number of applied cycles is illustrated. Fig. 16(a) and (b) present back-analyses of Test C2 and C3 respectively. Two displacement motions from each test are presented. Since pile head load was used as input in the analyses, pile head displacement was calculated. The calculated deflection and bending moment profiles compare generally very well with the measured response, demonstrating the predictive capability of the model.

3.4. SOLCYP centrifuge model testing

Khemakhem [14] reports a comprehensive set of centrifuge model tests of piles in Kaolin clay under monotonic and cyclic lateral loading. Those tests formed part of the SOLCYP project, which is summarized in Puech and Garnier [22]. Selected monotonic and cyclic tests carried out in slightly over-consolidated Kaolin were back-analysed using the currently proposed model. The details of the tests and back-analyses are presented below.

3.4.1. Geometry and instrumentation

The model tests were carried out at the IFSTTAR centrifuge facility. All the tests were run at 50 g. Table 3 summarizes the geometries of the model pile and dimensions used in back-analysis.

In the discussions and back analyses presented below, unless otherwise stated, all dimensions refer to prototype scale. The model pile is instrumented with 21 levels of strain gauges to measure the bending moment along the pile. The gauges are evenly spaced vertically, 0.75 m (prototype scale) apart. The pile is loaded 2 m above the mudline, where the applied force and induced lateral displacement are measured.

3.4.2. Soil conditions

Two types of soil conditions were tested by Khemakhem [14], namely saturated, slightly over-consolidated clay and unsaturated, heavily over-consolidated clay. The back-analyses reported herein focus on tests carried out in the saturated, lightly over-consolidated clay. The tests were carried out on Kaolin clay. The soil sample was prepared from Kaolin slurry mixed under vacuum to 90% water content, consolidated at 1 g under a hydraulic press. To achieve the desired sample height, the sample was prepared in three layers. Before the pile tests, the sample was reconsolidated under 50 g in-flight. The undrained shear strength (s_u) was established from in-flight cone penetration test using the empirical correlation presented by Garnier [9].

$$s_u = q_c/18.5 \quad (3)$$

where q_c is the measured cone resistance.

It is unclear which shear mode the correlated shear strength corresponds to and in the back-analyses, it is assumed to represent an average strength, which is typically similar to the DSS strength. Considerable variation within a soil sample and across different soil samples were revealed by the in-flight CPT tests, as illustrated in Fig. 17. Khemakhem [14] attributed the variation to the inadequate pressure control of the hydraulic press that was used to prepare the soil samples at 1 g. Based on the results measured in four samples, low and high estimate profiles are drawn. In the Figure, the representative profile suggested by Khemakhem [14] is also illustrated for comparison. In the back-analysis below, except for the chosen monotonic test, it was unfortunately not possible to identify the test specific shear strength

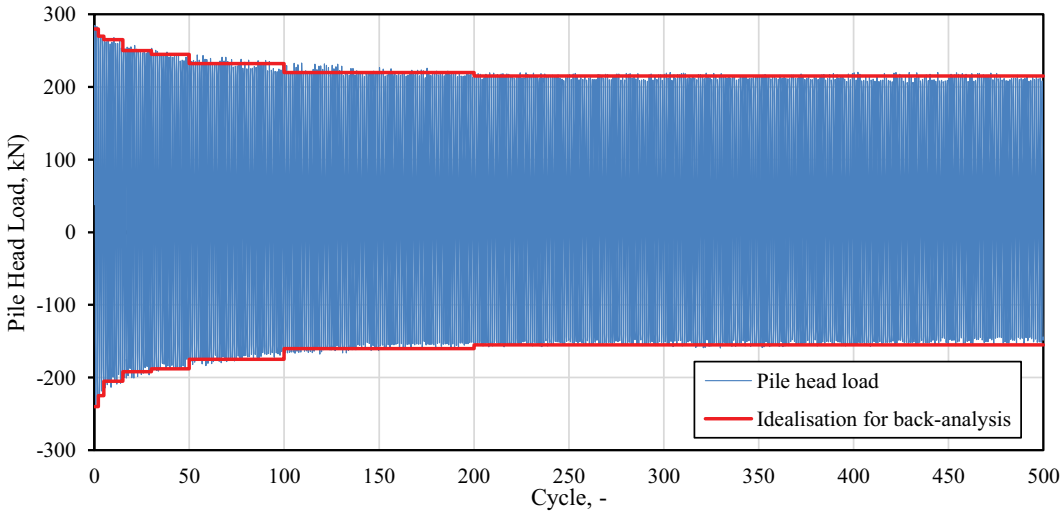

Fig. 15. Evolution of pile head lateral load during displacement controlled cyclic loading and idealisation for back analysis (example shown for C2M3).

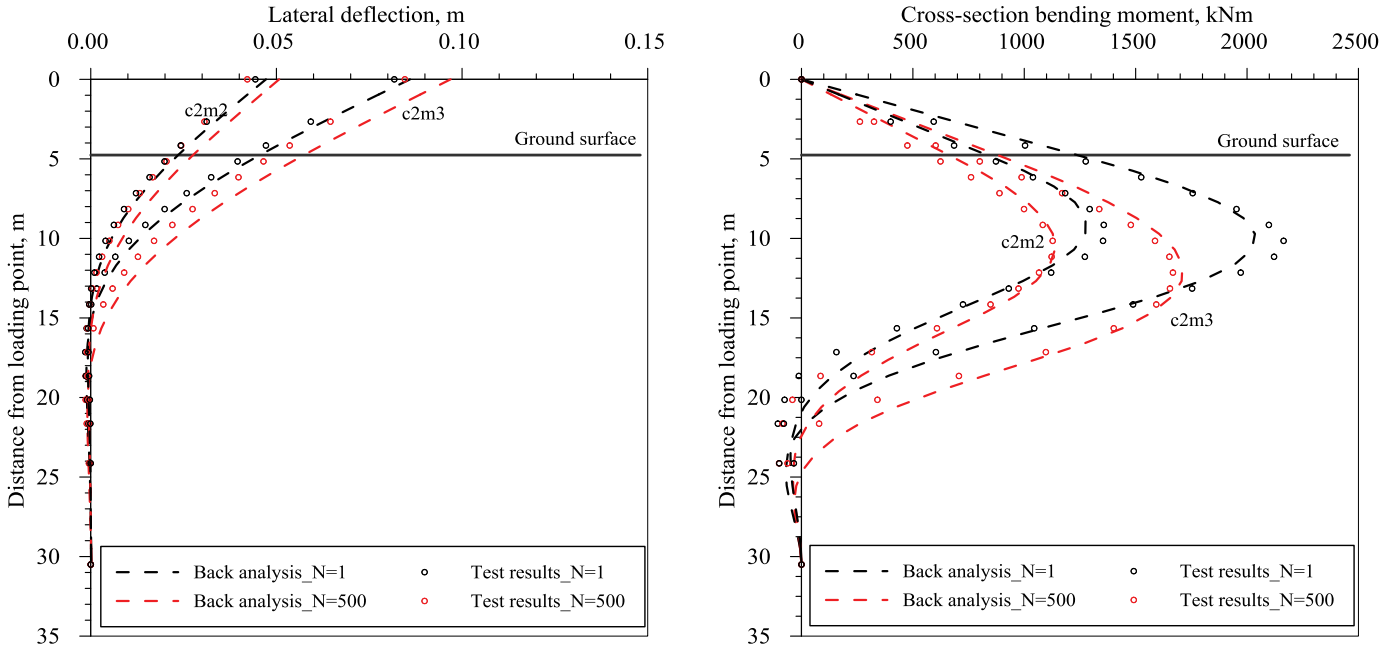

(a) Test C2

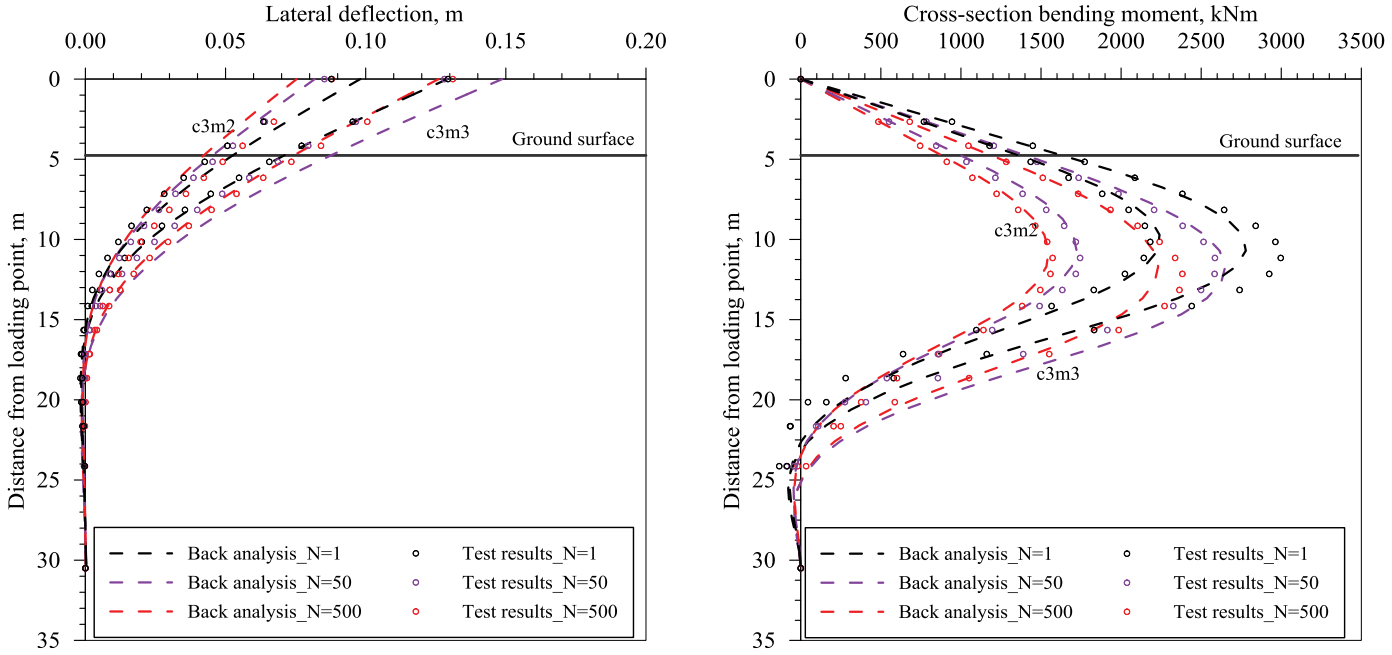

(b) Test C3

Fig. 16. Back analysis of Zakeri et al. [25] cyclic tests.

profile. All the back-analyses presented below were performed using representative profile suggested by Khemakhem [14]. However, the variation of the strength profile should be borne in mind when evaluating the results of the back-analyses. Fig. 17 also presents the estimated over-consolidation ratio (OCR) based on the stress history applied to soil during sample preparation.

For the back-analyses, a fully rough soil-pile interface roughness factor was assumed. In addition, the interface is allowed to gap freely, which is consistent with the observation in the tests.

The soil response of the Kaolin clay under monotonic and cyclic loading is already summarized in Section 3.3. However, those tests were for normally consolidated Kaolin. Based on Fig. 17, the SOLCYP soil samples have OCR greater than 1. As discussed previously, a soil with an OCR greater than one generally exhibits more ductile response than normally consolidated soil under monotonic loading, and more rapid degradation under cyclic loading. In the back analyses, the OCR effect is accounted for in an approximate manner due to lack of tests data for kaolin at OCR greater than one. Based on the trend illustrated

Table 3
Summary of pile geometry in model scale and prototype scale.

Parameter	Model scale	Prototype scale (used in back analyses)
Total pile length	360 mm	18 m
Penetrated length	320 mm	16 m
Diameter	18 mm	0.954 m*
E, GPa (Aluminium)	74	74
Wall thickness	1 mm	40 mm*

* The pile diameter and the wall thickness do not scale proportionally to the g level as the coating on the strain gauges enlarge the pile diameter by 6% [14].

in Fig. 8, correction factors were evaluated. For the depth interval (0–6.6 m), an average OCR = 4 is assumed and an OCR = 2 is assumed for deeper soils. For OCR = 4, the G_{50}/s_{uD} ratio is reduced to approximate 40% of that for OCR = 1, which implies a stiffness reduction factor of 2.5. For OCR = 2, the G_{50}/s_{uD} ratio is reduced to approximate 70% of that for OCR = 1, which implies a stiffness reduction factor of 1.4. These stiffness reduction factors were applied to scale up the strains in the cyclic contour diagrams (for both the average and the cyclic strain components). The effect of OCR on the normalised monotonic p-y curve is illustrated in Fig. 17.

3.4.3. Pile installation and loading

The model pile was installed at 1 g. A slightly oversized hole was first created by a manually operated auger. The test pile is then placed into the predrilled hole. The small clearance between the pile shaft and the soil at the surface is closed by hand. The clearance below the mudline is assumed to be closed by self-weight of the soil when it is ramped up and reconsolidated under 50 g.

The pile head load is applied 2 m above the mudline. The monotonic tests were run in displacement-controlled mode at a constant velocity of 0.4 mm/s (model scale) or 20 mm/s at prototype scale. At this displacement rate, 10% pile diameter is reached within 4.8 s. This is approximately three orders of magnitude faster than a standard monotonic DSS test. Significant rate effect is expected. This point will be further discussed in the result section.

The cyclic tests were run in load-controlled mode, where sinusoidal load history was applied to the pile head. For tests run with a non-zero average horizontal load, the loading consists of two phases:

- Phase 1: application of the average load. This was applied at a speed of 0.02 kN/s (model scale) or 50 kN/s in prototype scale. Again, this is an extremely fast loading speed, compared to a monotonic pile capacity of 220 kN at 10% of a diameter pile head deflection. While this average load is held during the cyclic pile testing, pile head deflection due to the average loading is expected to increase with time due to creep. This aspect will be further discussed below.
- Phase 2: application of the cyclic horizontal load. All the tests were run with a frequency of 0.25 Hz, i.e. a loading period of 4 s.

3.4.4. Back-analysis of monotonic test

One monotonic lateral pile load test was back analysed. For this selected test, the soil strength profile is reported in Khemakhem [14], which corresponds to the "Representative profile Khemakhem [14]" shown in Fig. 17. As mentioned above, the shear strain rate experienced by the soil during the monotonic pile test far exceeded the strain rate applied in the monotonic DSS tests. In the back analysis, a 25% increase in mobilised soil strength is assumed to account for the rate effect. This rate effect correction is in the low range of the rate effect data base

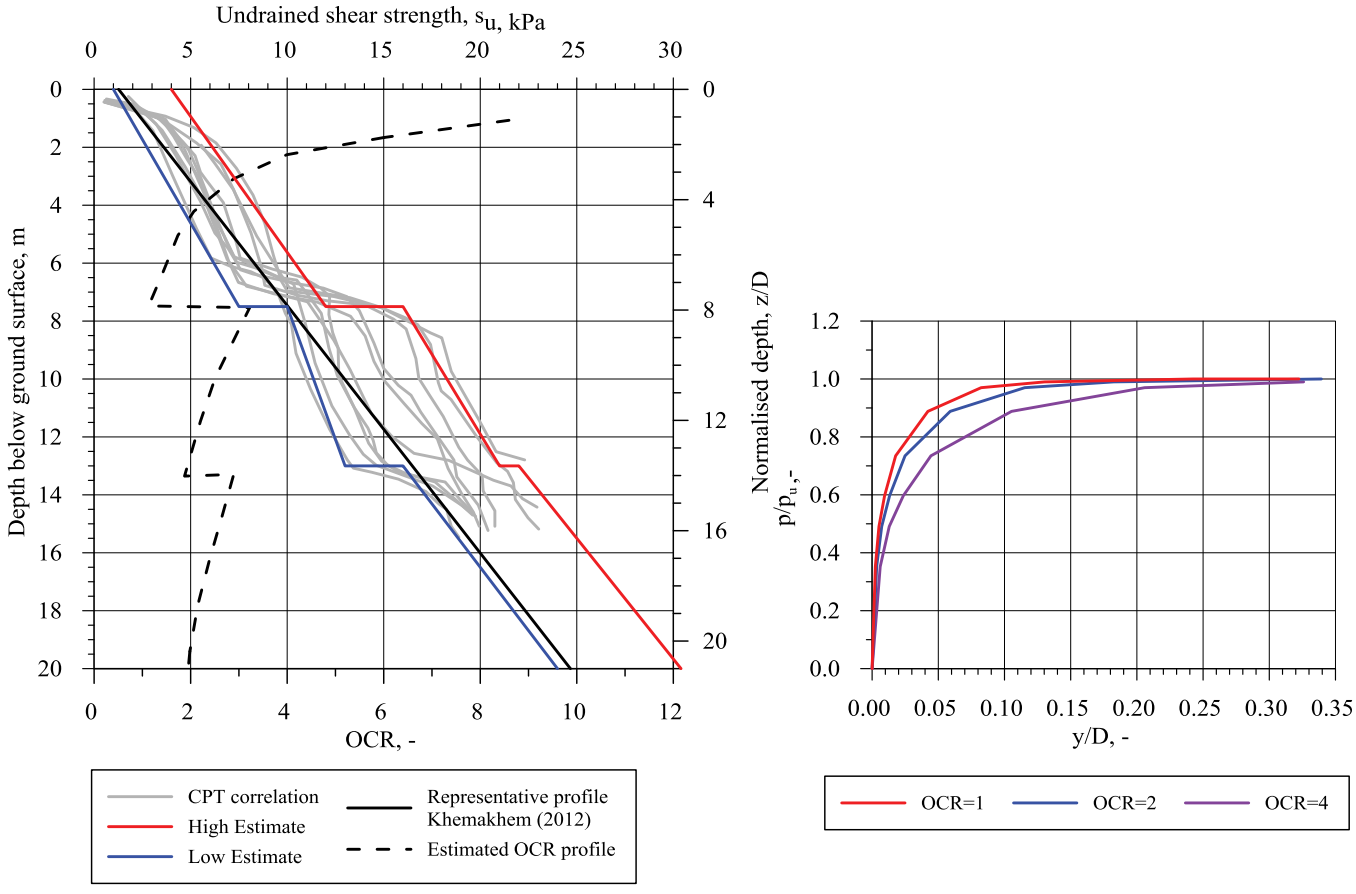

Fig. 17. Low and high estimate undrained shear strength, OCR versus depth and monotonic p-y curves for different OCR values.

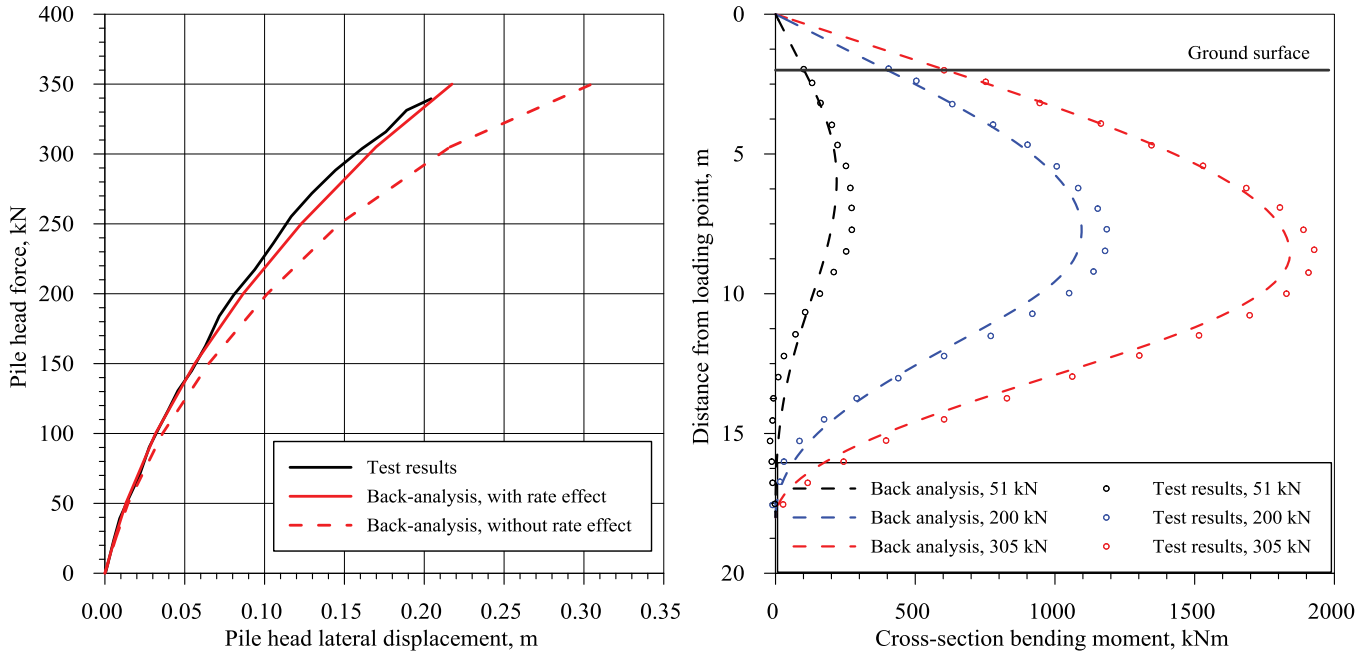

Fig. 18. Comparison of bending moment profile for monotonic test SOLCYPC05S1ins.

presented by Lunne and Andersen [18]. Fig. 18 presents the comparison of the measured pile head load-displacement curve against the back-analyses, with and without consideration of the rate effect and shows that the analysis without considering the rate effect under-predicts the system stiffness. The match is much improved when the rate effect is taken into consideration. Fig. 18 also illustrates the comparison of the bending moment profile along the pile between the physical measurements and the back-analysis (with consideration of the rate effect) at three different load levels. Again, a good match is demonstrated.

3.4.5. Back-analyses of cyclic tests

Two cyclic pile tests reported by Khemakhem [14] were chosen for back-analysis. The details of the two tests are summarized in Table 4. The two tests have the same average lateral load level (150 kN), but different cyclic amplitudes. Test C09S1ins has a large cyclic amplitude and the load direction is reversed during each cycle, while test C10S1ins has a relatively small cyclic amplitude and the lateral load does not reverse direction during cycling.

Figs. 19 and 20 present the results of back-analysis for test C09S1ins. Fig. 19 compares back-analysed and the measured the bending moment profile along the pile length in the 10th cycle. A reasonably good match is demonstrated, although the back-analysis predicts slightly higher bending moment. It is noted that near the ground surface, the back-analysis already suggests slightly higher bending moment, which may indicate that the applied load in the physical test is possibly smaller than 350 kN. Fig. 20 compares the evolution of pile head deflection and maximum bending moment along the pile with the number of applied load cycles. The back-analysis predicts a similar trend to the experimental observation. However, towards the end of the test, the experiment appears to exhibit accelerated increase in bending moment and pile head deflection, indicating imminent failure. The back-analysis however predicts more steady development of pile head deformations. In the figure, the back-analysis by Khemakhem [14], is also presented for information. In general, the current back-analysis performs better or similarly.

It is noted that at $N = 1$, the model predicts larger displacement than the test observation. This may be due to how the average load was applied in the test. As mentioned earlier, the average horizontal load was applied at 50 kN/s, at which only three seconds was needed to apply the average load in this test. However, in the cyclic DSS tests which were used to develop the contour diagram, the average shear stress was first applied to the soil sample and maintained for typically an hour before the cyclic shear stress was applied. The rate effect involved in the average loading phase of the pile test may have resulted in the initial stiffer response. During the continuous cycling, displacement due to the average lateral load gradually increases because of creep.

Figs. 21 and 22 present the results of back-analysis for test C10S1ins. Due to availability of test results reported in Khemakhem [14], the bending moment profile is compared between the current back analysis and the test results at $N = 100$ only. A very good match is demonstrated, although the maximum bending moment is slightly under-predicted. Fig. 22 compares the evolution of maximum bending moment along the pile and the pile head deflection with number of applied load cycles. The same general trend is observed, although the back analysis predicts lower maximum bending moment and smaller pile head deflection after many cycles. With continued cyclic loading, the pile response stabilises. It is again noted that at $N = 1$, the model predicts larger displacement than the test observation, which may be explained by how the average horizontal load was applied. In Fig. 21, the back-analysis by Khemakhem is also presented. In general, the current back-analysis performs better or similarly.

The back-analyses of the two cyclic tests illustrates that the cyclic model generally captures the trend revealed by the centrifuge tests, although some discrepancies are noted. As discussed in Section 3.4.2, uncertainties exist with the exact undrained shear strength profiles in the cyclic tests. Furthermore, the effect of tension gapping, which causes an apparent degradation of the soil-pile interaction stiffness due to permanent soil displacement, as discussed in Section 3.2.5, is also likely to have contributed to the difference between model prediction and the test measurements.

Table 4
Two SOLCYP cyclic pile tests chosen for back-analysis.

Test name	Average load, kN	Cyclic load, kN	No. of cycles
C09S1ins	150	200	40
C10S1ins	150	50	1000

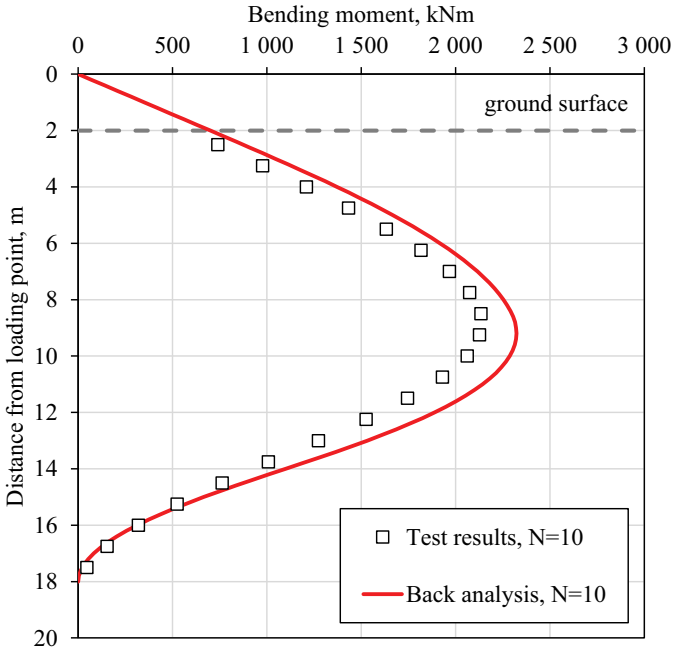

Fig. 19. Comparison of the bending moment profile at 10th load cycle during test C09S1ins.

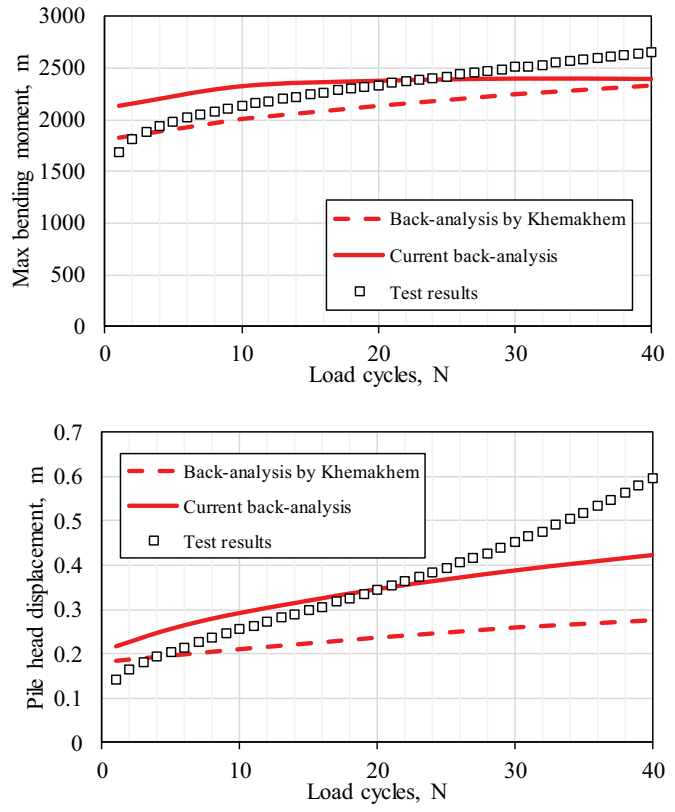

Fig. 20. Evolution of pile head displacement and maximum bending moment with no. of applied load cycles during test C09S1ins.

4. Concluding remarks

This paper presented verification of a framework for analysing the pile response under cyclic lateral loading. The framework is based on fundamental soil performance measured at soil element level. It allows for consideration of site-specific cyclic soil properties, including effects

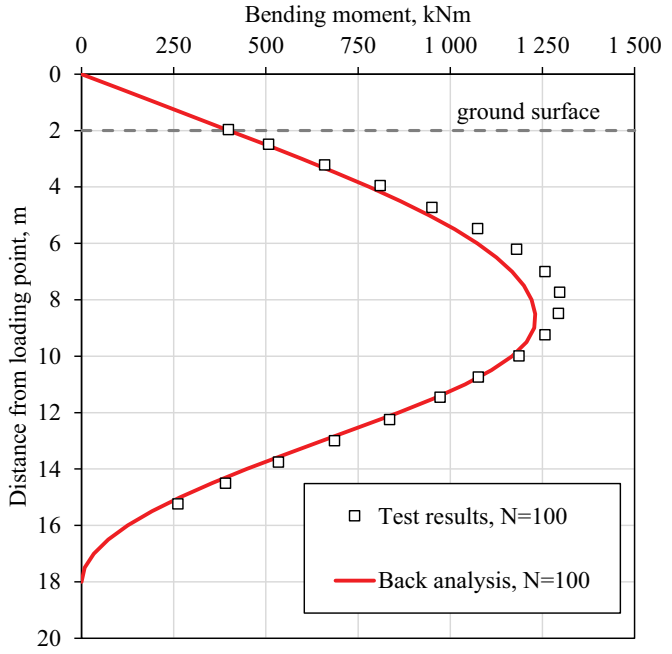

Fig. 21. Comparison of the bending moment profile at 100th load cycle during test C10S1ins.

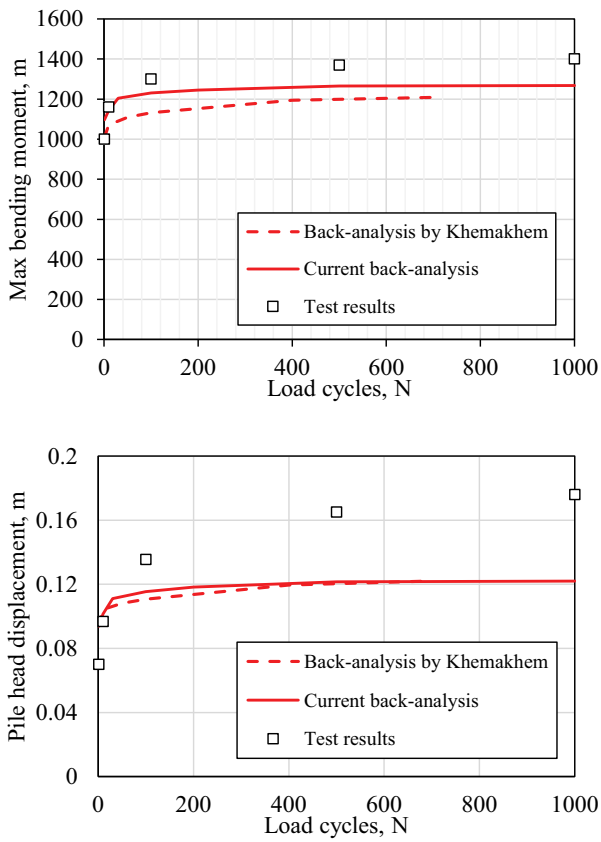

Fig. 22. Evolution of pile head displacement and maximum bending moment with no. of applied load cycles during test C10S1ins.

of over-consolidation ratio, rate of loading and strength anisotropy, as well as interface roughness, gapping and project specific cyclic loading characteristics into the pile foundation design. This is a step-change improvement from current codes and standards recommendations which are based on a series of tests on a single pile at a single site (the

Sabine River tests). The framework was used in the back-analyses of four series of model/centrifuge pile tests (although only three test series were reported in this paper) which demonstrated its ability to capture the essential behaviour of pile foundations under cyclic lateral loading and its potential for application in the design of long slender piles for offshore platforms.

CRediT authorship contribution statement

Youhu Zhang: Conceptualization, Methodology, Software, Validation, Investigation, Writing - original draft. **Knut H. Andersen:** Conceptualization, Resources, Investigation, Writing - review & editing. **Philippe Jeanjean:** Conceptualization, Resources, Investigation, Writing - review & editing.

Declaration of Competing Interest

The authors declare that they have no known competing financial interests or personal relationships that could have appeared to influence the work reported in this paper.

Acknowledgements

The authors gratefully acknowledge the funding from BP America and from an NGI internal research project funded by the Norwegian Research Council. The authors would also like to acknowledge the help from Dr Meriam Khemakhem regarding the SOLCYP centrifuge testing data. Lastly, the authors are grateful to their respective companies for permission to publish.

Supplementary materials

Supplementary material associated with this article can be found, in the online version, at doi:10.1016/j.apor.2020.102085.

References

[1] K.H. Andersen, A. Kleven, D. Heien, Cyclic soil data for design of gravity structures, ASCE J. Geotech. Eng. 114 (5) (1988) 517–539.
[2] K.H. Andersen, P. Jeanjean, D. Luger, H.P. Jostad, Centrifuge tests on installation of suction anchors in soft clay, Ocean Eng. 32 (7) (2005) 845–863.
[3] K.H. Andersen, Cyclic soil parameters for offshore foundation design. The third ISSMGE McClelland lecture, in: V Meyer (Ed.), Proc. Int. Symp. Frontiers in Offshore Geotechnics, ISFOG 2015, Taylor and Francis, London, 2015, pp. 5–82 Revised version in: http://www.issmge.org/committees/technical-committees/applications/offshore and click on “Additional Information”.
[4] API RP 2A 3rd Edition, Recommended Practice for Planning, Designing and Constructing Fixed Offshore Platforms, Published by the American Petroleum Institute, 1972 January.
[5] API Recommended Practice 2GEO, Geotechnical and Foundation Design Considerations, 1st Edition Addendum 1, Published by the American Petroleum Institute, 2014 April 2014.
[6] B. Byrne, R. McAdam, H. Burd, G. Houlsby, C. Martin, L. Zdravkovic, D. Taborda, D. Potts, R. Jardine, M. Sideri, F.C. Schroeder, K. Gavin, P. Doherty, D. Igoe, A. Muir Wood, D. Kallehave, J.K. Gretlund, New design methods for large diameter piles under lateral loading for offshore wind applications, 3rd International Symposium on Frontiers in Offshore Geotechnics (ISFOG 2015), Oslo, Norway. 2015, 2015, pp. 705–710.
[7] P. Carotenuto, A. Carraro, Y. Guadalupe-Torres, R. Dyvik, K.H. Andersen, L. Andresen, M.J. Cassidy, Characterization of kaolin clay under cyclic loading by element testing, ASTM Geotech. Testing J. (2020) under preparation.
[8] C.T. Erbrich, M.P. O'Neill, P. Clancy, M.F. Randolph, Axial and lateral pile design in carbonate soils, Proc., 2nd International Symposium on Frontiers in Offshore Geotechnics (ISFOG II), 2010, pp. 125–154.
[9] J. Garnier, Modèles physiques en géotechnique I—Evolution des techniques expérimentales et des domaines d'application, Rev. Française Géotech. 97 (2001) 3–29.
[10] P. Jeanjean, Re-assessment of p-y curves for soft clays from centrifuge testing and finite element modelling, OTC 20158, Proc. Offshore Tech. Conf. Houston, USA, 2009.
[11] P. Jeanjean, Y. Zhang, A. Zakeri, K.H. Andersen, R. Gilbert, A. Senanayake, A framework for monotonic p-y curves in clays, Keynote Lecture, OSIG SUT Conference, 2017, London, 2017.
[12] H.P. Jostad, G. Grimstad, K.H. Andersen, M. Saue, Y. Shin, D. You, A FE procedure for foundation design of offshore structures – applied to study a potential OWT monopile foundation in the Korean Western Sea, Geotech. Eng. J. SEAGS AGSSEA 45 (4) (2014) 63–72.
[13] K. Karlsrud, T. Haugen, Cyclic loading of piles and pile anchors – field model tests final report: summary and evaluation of test results, (1983) NGI report 40010-28, dated April 18, 1983.
[14] M. Khemakhem, Etude Experimentale de la Réponse aux Charges Latérales Monotones et Cycliques d'un Pieu Fore Dans L'argile, PhD thesis Ecole Centrale de Nantes, France, 2012.
[15] C.C. Ladd, R. Foott, New design procedure for stability of soft clays, J. Geotech. Eng. Div. 100 (7) (1974) 763–786.
[16] E. Liedtke, K.H. Andersen, Y. Zhang, P. Jeanjean, Monotonic and cyclic soil properties of Gulf of Mexico clays, Offshore Technology Conference, OTC-29622-MS, 2019.
[17] H.E. Low, T. Lunne, K.H. Andersen, M.A. Sjursen, X. Li, M.R. Randolph, Estimation of intact and remoulded undrained shear strengths from penetration tests in soft clays, Geotechnique 60 (11) (2010) 843–859.
[18] T. Lunne, K.H. Andersen, Soft clay shear strength parameters for deepwater geotechnical design, Keynote Lecture, 6th OSIG SUT Conference, 2007, London, UK, 2007, pp. 151–176.
[19] H. Matlock, R.L. Tucker, Lateral Load Tests of an Instrumented Pile at Sabine, Report to Shell Development Company, Texas, 1961 September 15, 1961.
[20] H. Matlock, Correlations For Design of Laterally Loaded Piles in Soft Clay, Report to Shell Development Company, 1962 September 15, 1962.
[21] H. Matlock, Correlations for design of laterally loaded piles in soft clays, Offshore Technology Conference, Houston, Texas, OTC 1204, 1970.
[22] A. Puech, J. Garnier, Design of Piles Under Cyclic Loading: SOLCYP Recommendations, Wiley-ISTE, 2017 ISBN: 978-1-119-46894-3, Nov 2017.
[23] P.J. Vardanega, B.H. Lau, S.Y. Lam, S.K. Haigh, S.P.G. Madabhushi, M.D. Bolton, Laboratory measurement of strength mobilisation in kaolin: link to stress history, Geotech. Lett. 2 (2012) 9–15 2012.
[24] D.J. White, C. Gaudin, N. Boylan, H. Zhou, Interpretation of T-bar penetration tests at shallow embedment and in very soft soils, Can. Geotech. J. 47 (2010) 218–229.
[25] A. Zakeri, E.C. Clukey, E.B. Kebadze, P. Jeanjean, Fatigue analysis of offshore well conductors: part I—Study overviewand evaluation of series 1 centrifuge tests in normally consolidated tolightly over-consolidated kaolin clay, Appl. Ocean Res. 57 (2016) (2016) 78–95.
[26] Y. Zhang, K.H. Andersen, R.T. Klinkvort, H.P. Jostad, N. Sivasithamparam, N.P. Boylan, T. Langford, Monotonic and cyclic p-y curves for clay based on soil performance observed in laboratory element tests, Offshore Technology Conference, Houston, Texas. OTC 26942, 2016.
[27] Y. Zhang, K.H. Andersen, G. Tedesco, Ultimate bearing capacity of laterally loaded piles in clay - Some practical considerations, Mar. Struct. 50 (2016) (2016) 260–275.
[28] Y. Zhang, K.H. Andersen, P. Jeanjean, A. Mirdamadi, A.S. Gundersen, H.P. Jostad, A framework for cyclic p-y curves in clay and application to pile design in GoM, OSIG SUT Conference, 2017, London, 2017.
[29] Y. Zhang, K.H. Andersen, Scaling of lateral pile p-y response in clay from laboratory stress-strain curves, Mar. Struct. 53 (2017) (2017) 124–135.
[30] Y. Zhang, K.H. Andersen, P. Jeanjean,, K. Karlsrud, T. Haugen, Validation of a monotonic and cyclic p-y framework by lateral pile load tests in a stiff over-consolidated clay at the Haga site, ASCE J. Geotech. Geoenviron. Eng. (2020) 2020, under review.
[31] Y. Zhang, K.H. Andersen, P. Jeanjean, Cyclic p-y curves in clays for offshore structures, Offshore Technology Conference, Houston, USA, OTC-29346-MS, 2020.
[32] Y. Zhang, K.H. Andersen, Soil reaction curves for monopiles in clay, Mar. Struct. 65 (2019) (2019) 94–113.
[33] B. Zhu, Z.J. Zhu, T. Li, J.C. Liu, Y.F. Liu, Field tests of offshore driven piles subjected to lateral monotonic and cyclic loads in soft clay, J. Waterw. Port Coast. Ocean Eng. 143 (5) (2017) 05017003.617, , https://doi.org/10.1061/(ASCE)WW.1943-5460.0000399.